1 October 2001

OPTICS COMMUNICATIONS

Optics Communications 197 (2001) 385–391

www.elsevier.com/locate/optcom

10-GHz actively mode-locked pulse generation employing a semiconductor optical amplifier and an electroabsorption modulator in a fiber ring

Jianfeng Zhang *, Minyu Yao, Hongming Zhang, Qianfan Xu, Yizhi Gao

Department of Electronic Engineering, Tsinghua University, Beijing 100084, China

Received 30 April 2001; received in revised form 4 June 2001; accepted 22 July 2001

Abstract

A 10-GHz fiber-integrated ring laser incorporating a semiconductor optical amplifier and an electroabsorption modulator was investigated both theoretically and experimentally. The time-domain *ABCD* law was employed to clarify the impacts of optical elements on the mode-locked pulses. The obtained analytical results were testified by the experimental ones. Such a ring laser also showed good performance as an optical pulse source, which generated a stable pulse train with a pulse width of 10 ps and a tunable wavelength range of 30 nm. © 2001 Elsevier Science B.V. All rights reserved.

Keywords: Fiber ring laser; Actively mode locking; Electroabsorption modulator; Semiconductor optical amplifier

1. Introduction

Ultrashort pulse sources with a high repetition rate are key components in the optical time division multiplexing (OTDM) system. They are also essential for optical signal processing, long distance soliton transmission, etc. Until now, various techniques have been demonstrated to generate optical pulses, such as erbium doped fiber laser (EDFL), gain-switched laser, and electroabsorption (EA) modulator. EA modulator is very attractive as the optical pulse source due to its compactness, robustness and other merits. However, it has shown that direct modulation of EA modulator usually cannot generate the pulses whose extinction ratio and duty ratio are sufficient for the OTDM applications [1,2]. To further improve the performance, several methods have been proposed, such as the use of tandem connected modulators [4], adiabatic compression of the output pulses [6].

Alternatively, Guy et al. incorporated an EA modulator in a semiconductor fiber ring laser, firstly showing that such a simple configuration could generate optical pulses as short as 3.0 ps [3]. Dong further investigated the short-term stability of a similar configuration, demonstrating its relaxation-free characteristics [5]. In that ring laser setup, a $LiNbO_3$ modulator was incorporated instead of EA modulator and the generated pulse

* Corresponding author. Tel.: +86-10-6277-2370; fax: +86-10-6277-0317.

E-mail addresses: zhjf99@mails.tsinghua.edu.cn, jianfeng2000@263.net (J. Zhang).

0030-4018/01/$ - see front matter
PII: S0030-4018(01)01449-3

train is significantly chirped with a relatively wide pulse width.

However, the influences of semiconductor optical amplifier (SOA) gain dynamics and EA modulation characteristics on the generated pulses of such a fiber ring laser were scarcely referred in literature. In this paper, this topic was investigated both theoretically and experimentally. We employed the time-domain *ABCD* law to analyze the laser characteristics. The obtained results clarified the impact of EAM and SOA on the pulse duration and allowed us to optimize the laser performance in experiment. The output pulse train is stable, nearly transformed with a 10 ps FWHM and 30 nm wavelength tuning range.

2. Numerical model

The configuration of the fiber ring laser is shown in Fig. 1. A SOA was used as the gain medium, an EA modulator driven by 10-GHz RF electrical signal functioned as the amplitude modulator in the ring cavity.

We employed the time-domain *ABCD* law to analyze the laser characteristics. The temporal *ABCD* matrix formalism has been shown to be a useful tool to obtain a steady-state solution of output pulses from various mode-locked lasers [8,9]. Compared with other complex numerical models, it is very convenient for easy derivation of analytical solutions and for understanding pulses characteristics.

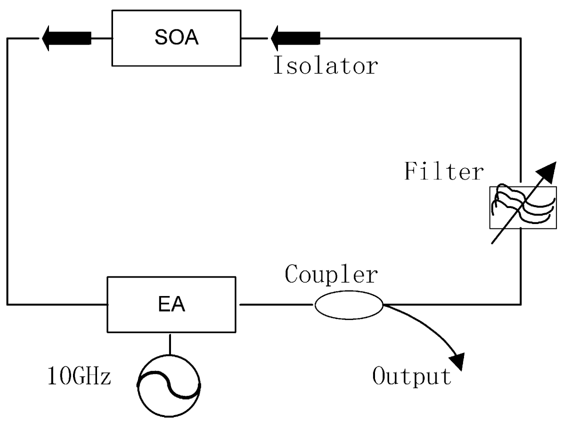

Fig. 1. Schematic diagram of laser configuration.

In all cases, the pulse shape was assumed to be Gaussian, which is defined by

$$E(t) = \sqrt{P_0}\exp\left[-\frac{t^2}{2\tau^2}(1+\mathrm{i}C)\right] \tag{1}$$

where P_0 is the peak power, τ is the $1/e$ pulse width, C is the linear chirp parameter. Thus the q parameter is defined by

$$\frac{1}{q} = \frac{1+\mathrm{i}C}{\tau^2} \tag{2}$$

When such a pulse passes through an optical element characterized by *ABCD* matrix $\begin{bmatrix} A & B \\ C & D \end{bmatrix}$, the q parameter at output will satisfy the following *ABCD* law

$$q_{\text{out}} = \frac{Aq_{\text{in}} + B}{Cq_{\text{in}} + D} \tag{3}$$

where q_{out} and q_{in} are the corresponding q parameter at output and input port.

In the following, the *ABCD* matrix corresponding to different elements in the ring laser were derived, and an analytical expression for the pulse duration was obtained.

As for the EA modulator, its modulation characteristics can be expressed by

$$T = \exp\left(-\left(\frac{V}{V_0}\right)^{\alpha}\right) \tag{4}$$

where T is transmission function, V is the modulation voltage, V_0 and α are parameters determining the modulation efficiency. For most EA modulators, α is close to 1.0. The *ABCD* matrix corresponding to EA modulator can be derived (see Appendix A):

$$T_{\text{EA}} = \begin{bmatrix} 1 & 0 \\ \frac{V_{\text{m}}}{2V_0}(2\pi f)^2 & 1 \end{bmatrix} \tag{5}$$

where V_{m} is the amplitude of modulation voltage, f is the repetition rate.

To derive the *ABCD* matrix of SOA, two assumptions were made:

1. Optical pulses keep their Gaussian shape when they pass through SOA.
2. The induced chirp in SOA is small, thus its interaction with optical filter do not introduce any waveform distortions.

Such assumptions are reasonable when the input pulse energy do not deeply saturate the SOA. The *ABCD* matrix of SOA is defined by (see Appendix A)

$$T_{\mathrm{SOA}} = \begin{bmatrix} 1 & 0 \\ -\dfrac{e^{h_{\mathrm{sat}}}(e^{h_{\mathrm{sat}}}-1)}{\pi f^2 \tau^2}\left(\dfrac{\overline{P}}{P_{\mathrm{sat}}\tau_{\mathrm{s}}}\right)^2 & 1 \end{bmatrix} \tag{6}$$

where

$$h_{\mathrm{sat}} = \frac{h_0}{1+\dfrac{\overline{P}}{P_{\mathrm{sat}}}}$$

$\overline{P}$ is the average power of the pulse input into SOA. P_{sat} is the saturation power, τ_{s} is the recovery time of carriers, h_0 is the small signal gain.

By using a parabolic approximation, the *ABCD* matrix for optical filter is defined by [4]

$$T_{\mathrm{filter}} = \begin{bmatrix} 1 & \dfrac{1}{B_{\mathrm{f}}^2} \\ 0 & 1 \end{bmatrix} \tag{7}$$

where B_{f} is related to the 3 dB bandwidth of filter B_{FWHM} by $B_{\mathrm{f}} = 2\pi B_{\mathrm{FWHM}}/2(\ln 2)^{1/2}$.

In all, the total *ABCD* matrix for the ring laser is

$$T_{\mathrm{R}} = T_{\mathrm{EA}} T_{\mathrm{filter}} T_{\mathrm{SOA}} \tag{8}$$

Substituting Eqs. (5)–(7) into Eq. (8), the *ABCD* matrix for the ring laser is derived,

$$T_{\mathrm{R}} = \begin{bmatrix} 1-\dfrac{H}{2\tau^2 B_{\mathrm{f}}^2} & \dfrac{1}{B_{\mathrm{f}}^2} \\ \dfrac{V_{\mathrm{m}}}{2V_0}(2\pi f)^2 - \dfrac{H}{2\tau^2} & 1 \end{bmatrix} \tag{9}$$

where

$$H = \frac{e^{h_{\mathrm{sat}}}(e^{h_{\mathrm{sat}}}-1)}{\pi f^2}\left(\frac{\overline{P}}{E_{\mathrm{sat}}}\right)^2$$

To obtain the steady-state solution, the self-consistent condition of q parameter should be satisfied,

$$q(0) = q(L) \tag{10}$$

where L is the cavity length.

Introducing Eqs. (2), (9) and (10) into Eq. (3), we can obtain the analytical expression for the output pulse width,

$$\tau = \sqrt{\frac{HB_{\mathrm{f}} + \sqrt{H^2B_{\mathrm{f}}^2 - \dfrac{4V_{\mathrm{m}}}{V_0}(2\pi f)^2(H-2)}}{\dfrac{2V_{\mathrm{m}}}{V_0}(2\pi f)^2 B_{\mathrm{f}}}} \tag{11}$$

As for the output pulse, the chirp parameter is estimated toughly to the first order at the pulse center,

$$C = -\frac{\alpha H}{2} \tag{12}$$

Thus for the Gaussian pulse, the time–bandwidth product is

$$\Delta t\,\Delta v = \frac{2\ln 2}{\pi}\sqrt{1+C^2} \tag{13}$$

The characteristics of the output pulse can be evaluated by Eqs. (11) and (13). From those equations, we can clarify the impacts of optical elements in the ring.

Fig. 2 shows the relation between the pulse width and the modulation depth of EA modulator. It can be seen that the output pulse width decreases as the ratio V_{m}/V_0 increased. For EA modulators, V_0 is of small value due to the high

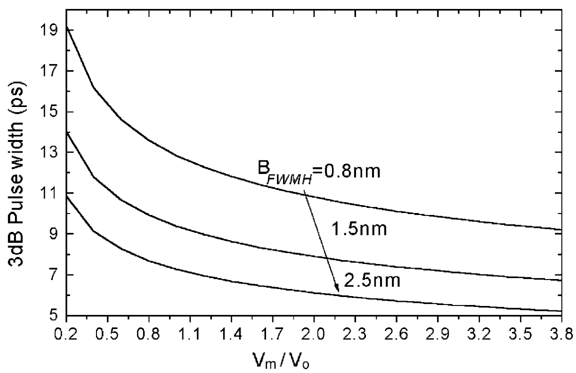

Fig. 2. Pulse width versus modulation depth (V_{m}/V_0) of EA modulator and the bandwidth of filter. In the calculation, the effect of gain saturation is neglected, $f = 10$ GHz.

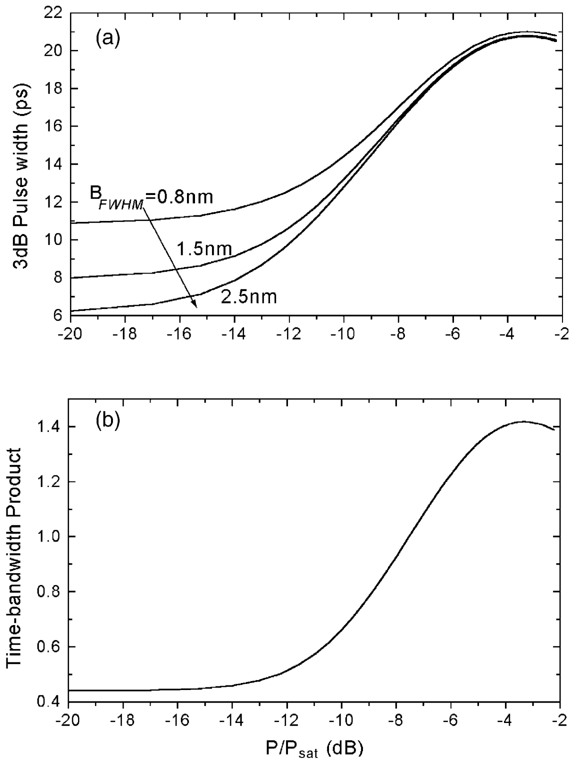

Fig. 3. The effect of gain saturation on (a) pulse width and (b) time–bandwidth product. In the calculation, $h_0 = 4.5$, $V_m/V_0 = 2.0$, $f = 10$ GHz, $\tau_r = 500$ ps.

modulation efficiency, therefore the ratio is usually larger than 2.0. Compared with other linear intensity modulators such as $LiNbO_3$, it is advantageous to employ EA modulator in the ring to generate short pulses. For a given modulation depth, the filter bandwidth determines the minimum pulse width. For example, the filter with a bandwidth larger than 2.5 nm should be employed to generate pulses as short as 5 ps.

In Fig. 3(a), gain saturation is shown to be an important factor resulting in the pulse broadening. As the ratio of average optical power in the ring versus the saturation power increased beyond 0.1, the pulse is broadened drastically. The gain saturation induced chirp also degrades the performance of the laser just as Fig. 3(b) shows. In all, we can conclude that it is necessary to adjust the parameters to prevent SOA being deeply saturated to get a high quality pulse train.

3. Experimental results and discussion

As shown in Fig. 1, the laser cavity was composed entirely from fiber-pigtailed devices. The EA modulator had a 3 dB electrical bandwidth of 10 GHz, and fiber-to-fiber insertion loss of 10 dB. Its modulation efficiency was measured as 7 dB/V, the corresponding V_0 parameter is equal to 1 V. Direct modulation on the EA modulator generated pulses with a minimum pulse width of 23 ps. The SOA has a fiber-to-fiber gain of 26 dB at the maximum current of 200 mA. Two Faraday isolators were placed either side of SOA to prevent the internal reflections and enable the unidirectional operation. The tunable optical filter had a 3 dB bandwidth of 1.5 nm.

In the experiment, both the injection current of SOA and modulation voltage of EA were finely adjusted. The RF frequency was also correspondingly tuned around 10 GHz to achieve the harmonic mode locking. When the small-signal-gain of SOA was adjusted to exactly compensate the linear loss in the cavity, and EA modulator was approximately biased and modulated to achieve the maximum value of V_m/V_0, this ring laser provided the optimum performance. This is in agreement with the theoretical predictions, which shows that EA modulator's nonlinear modulation characteristics contribute to the pulse compression mechanism in the ring, while the gain saturation effect in SOA results in the pulse broadening and chirping.

Fig. 4 shows the autocorrelation trace, optical waveform and optical spectrum of the pulse train obtained at 1547 nm. In Fig. 4(a), the trace is fitted by the autocorrelation of a Gaussian profile of 9.5 ps pulse width and shows a good fit. The measured trace is slightly asymmetric due to some unperfected alignments in the autocorrelator. The spectral FWHM is 0.42 nm, yielding the time–bandwidth product of 0.50. The related data were measured in the experiment, $G_0 = 15$ dB ($h_0 = 4.0$), $B_{FWHM} = 1.5$ nm, $V_m/V_0 = 2.5$, $P_{in}/P_{sat} = 0.1$. Introducing those data into expressions (11) and (13), the pulse width was calculated as 9.0 ps, and the time–bandwidth product as 0.48, which are generally in agreement with the experimental results. The optical waveform was also measured by

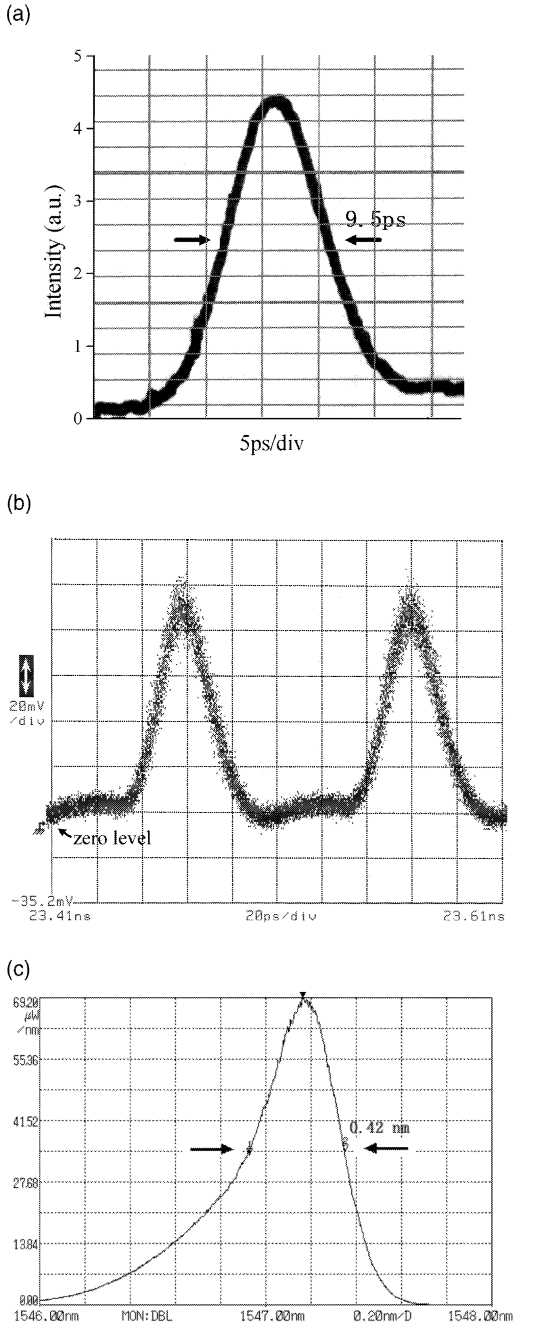

Fig. 4. (a) Autocorrelation trace, (b) waveform and (c) optical spectrum of output pulses.

a 20 GHz PIN detector and 45 GHz sampling oscilloscope (TEK11801C), indicating little intensity noise and timing jitter.

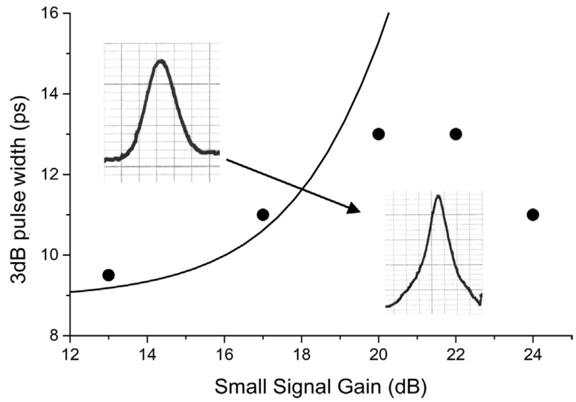

Fig. 5. The effect of gain saturation on the pulse width. The insets shows the corresponding autocorrelation trace at different gain level. Symbols denote the measurment data. The solid line is the theorectical curve calculated by Eq. (11).

Further investigation of the impact of SOA gain dynamics on the laser performance was also made. Fig. 5 shows the relation between the output pulse width versus the SOA's small signal gain. Both the experimental and theoretical results are shown in the diagram. In a certain range, the pulse width increased with the small signal gain level improving, just as Eq. (11) predicts. However, the pulse width decreased when the gain level was beyond 23 dB. The autocorrelation traces shown in Fig. 5 also indicate that the pulse shape deviated far from the Gaussian profile under this high gain level. These cannot be predicted by the proposed *ABCD* model. It is due to the fact that the SPM-induced chirp dominated and contributed to the pulse shaping, which is neglected in the proposed model. In this high gain regime, the output pulse train is highly chirped (spectral FWHM increased from 0.4 to 0.7 nm), which is not preferred for system applications.

Therefore, we expect to improve the pulse duration of laser output through the use of EA modulators with higher modulation efficiency and lower insertion loss, optical filter with broader bandwidth, and the SOA with higher saturation energy.

In the experiment, this laser also showed its good stability. Firstly, the total cavity can be considerably shortened by adopting SOA as the gain medium. Therefore it can be more insensitive to

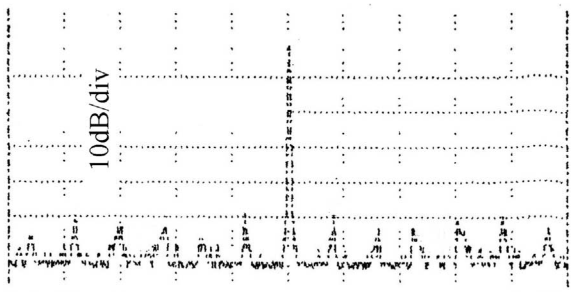

Fig. 6. RF spectrum of optical pulses.

the environmental perturbations. Without any active control, this kept stable for time scales of an hour. Furthermore, the laser also has a good short-term stability due to SOA's fast recovery time [5,12]. As Fig. 6 shows, the supermode noise in the laser have been suppressed below −50 dB. While in harmonically mode-locked EDFL, complex control and configuration have to be applied to reduce the supermode noise [10,11].

The wavelength tuning range of the laser was investigated by adjustment of the tunable filter. Due to the broad optical bandwidth of SOA and EA modulator, the tuning range was mainly determined by the filter. In this case, 10–12 ps pulses were generated over the range of 1530–1560 nm.

4. Conclusion

The fiber ring laser incorporating an EA modulator and SOA was investigated both theoretically and experimentally. The influences of SOA gain dynamics and EA modulator characteristics on the laser performance were clarified. Such a fiber ring also manifested much merit in the experiment, such as its robustness to generate short pulses, good short-term stability, broadband wavelength tunability, which make it a promising component for the high bit rate system.

Acknowledgement

This work is supported by Natural Science Foundation Committee of China (No. 60077001).

Appendix A. Derivation of *ABCD* matrix for EA modulator and SOA

In this appendix, we will derive *ABCD* matrix for EA modulator and SOA. The optical field is defined by

$$u(t) = \sqrt{P_0}\exp\left[-\frac{t^2}{2q}\right] \quad (A.1)$$

The EA modulator is sinusoidally driven by the RF electrical voltage,

$$V(t) = V_b + V_m\cos(2\pi ft) \quad (A.2)$$

where V_b is the bias voltage, V_m is the amplitude of modulation voltage. At the pulse center ($t = 0$), the following approximation can be applied,

$$\cos(2\pi ft) \cong 1 - \tfrac{1}{2}(2\pi f)^2 t^2 \quad (A.3)$$

Introducing Eqs. (A.1)–(A.3) into Eq. (3), the output optical field can be expressed by

$$u_{EA}(t) = u(t)\exp\left(-\frac{V_b + V_m\cos(2\pi ft)}{V_0}\right)$$
$$\approx \sqrt{P_0}\exp\left(-\frac{V_b}{V_0}\right)\exp\left(-\frac{t^2}{2q} - \frac{V_m}{2V_0}\frac{1}{2}(2\pi f)^2 t^2\right) \quad (A.4)$$

Thus the q parameter at output of EA is

$$\frac{1}{q_{out}} = \frac{1}{q} + \frac{V_m}{2V_0}(2\pi f)^2 \quad (A.5)$$

the *ABCD* matrix for EA can be derived,

$$T_{EA} = \begin{bmatrix} 1 & 0 \\ \frac{V_m}{2V_0}(2\pi f)^2 & 1 \end{bmatrix} \quad (A.6)$$

As for the SOA, the amplified optical field will be changed as follows:

$$u_{SOA}(t) = u(t)\exp\left(\frac{h(t)}{2}\right) \quad (A.7)$$

where $h(t)$ is time-dependent power gain coefficient of SOA, it satisfy the following equation [7],

$$\frac{dh}{dt} = \frac{h - h_0}{\tau_r} + (e^h - 1)\frac{|u(t)|^2}{P_{sat}\tau_r} \quad (A.8)$$

$h(t)$ can be expanded into second-order Taylor series at the $t = 0$,

$$h(t) = h(t=0) + h'(t=0)t + \tfrac{1}{2}h''(t=0)t^2$$

thus the q parameter at output of SOA is

$$\frac{1}{q_{\text{out}}} = \frac{1}{q} - \frac{h''(t=0)}{2} \tag{A.9}$$

In practice, the optical pulse is short that SOA has no time to recover during its duration, the first term of right-hand side of Eq. (A.8) can be neglected, the second order of $h(t)$ can be derived,

$$\frac{\mathrm{d}^2 h}{\mathrm{d}^2 t} = \mathrm{e}^h(\mathrm{e}^h - 1)\left(\frac{P(t)}{P_{\text{sat}}\tau_{\text{r}}}\right)^2$$

Thus at the pulse center ($t = 0$),

$$h''(t=0) = \mathrm{e}^{h_{\text{sat}}}(\mathrm{e}^{h_{\text{sat}}} - 1)\left(\frac{P_0}{E_{\text{sat}}}\right)^2 \tag{A.10}$$

where $h_{\text{sat}} = h_0/(1 + (\overline{P}/P_{\text{sat}}))$, $\overline{P}$ is average power of the pulse train. For the Gaussian profiled pulses, the relation between the peak power and the average power is as followed:

$$P_0 = \frac{\bar{P}}{\sqrt{\pi} f \tau} \tag{A.11}$$

Substituting Eqs. (A.10) and (A.11) we obtain the *ABCD* matrix for SOA:

$$T_{\text{SOA}} = \begin{bmatrix} 1 & 0 \\ -\dfrac{\mathrm{e}^{h_{\text{sat}}}(\mathrm{e}^{h_{\text{sat}}} - 1)}{\pi f^2 \tau^2}\left(\dfrac{\overline{P}}{P_{\text{sat}}\tau_{\text{s}}}\right)^2 & 1 \end{bmatrix} \tag{A.12}$$

References

[1] D.G. Moodie, M.J. Harlow, M.J. Guy, S.D. Perrin, C.W. Ford, M.J. Robertson, Discrete electronabsorption modulators with enhanced modulation depth, J. Lightwave Technol. 14 (1996) 2035–2042.

[2] O. Saeko, N. Koji, H. Hideaki, Low-drive-voltage MQW electroabsorption modulator for optical short-pulse generation, IEEE J. Quant. Electron. 28 (1992) 277–281.

[3] M.J. Guy, J.R. Taylor, D.G. Moodie, A.E. Kelly, 10 GHz 3 ps actively mode-locked ring laser incorporating a semiconductor laser amplifier and an electroabsorption modulator, Electron. Lett. 32 (1996) 2240–2241.

[4] D.D. Marcenac, A.D. Ellis, D.G. Moodie, 80 Gbit/s OTDM using electroabsorption modulators, Electron. Lett. 34 (1998) 101–103.

[5] D.H. Kim, S.H. Kim, Y.M. Jhon, Y.T. Byun, J.C. Jo, S.S. Choi, Ultrahigh-speed fiber-integrated semiconductor ring laser, Opt. Commun. 185 (2000) 381–385.

[6] P.C. Reeves-Hall, S.A.E. Lewis, S.V. Chernikov, J.R. Taylor, Picosecond soliton pulse-duration-selectable source based on adiabatic compression in Raman amplifier, Electron. Lett. 36 (2000) 622–624.

[7] G.P. Agrawal, N.A. Olsson, Self-phase modulation and spectral broadening of optical pulses in semiconductor-laser amplifiers, IEEE J. Quant. Electron. 25 (1989) 2297–2306.

[8] M. Nakazawa, H. Kubota, A. Sahara, K. Tamura, Time-domain *ABCD* matrix formalism for laser mode-locking and optical pulse transmission, IEEE J. Quant. Electron. 34 (1998) 1075–1081.

[9] Y. Li, C. Lou, G. Chang, Y. Gao, Theoretical study on the actively mode-locked fiber laser with the q parameter and the *ABCD* law, IEEE Photon. Technol. Lett. 11 (1999) 1590–1592.

[10] X. Shan, D.M. Spirit, Novel method to suppress noise in harmonically mode-locked erbium fibre laser, Electron. Lett. 29 (1993) 979–981.

[11] Y. Li, C. Lou, J. Wu, B. Wu, Y. Gao, Novel method to simultaneously compress pulses and suppress supermode noise in actively mode-locked fiber ring laser, IEEE Photon. Technol. Lett. 10 (1998) 1250–1252.

[12] F. Girardin, G. Guekos, A. Houbavlis, Gain recovery of bulk semiconductor optical amplifiers, IEEE Photon. Technol. Lett. 10 (1998) 784–786.